# Isoprenoid Biosynthesis as a Drug Target: Bisphosphonate Inhibition of *Escherichia coli* K12 Growth and Synergistic Effects of Fosmidomycin

Annette Leon,[†] Lei Liu,[‡] Yan Yang,[§] Michael P. Hudock,[†] Patrick Hall,[||] Fenglin Yin,[†] Danielle Studer,[⊥] Kia-Joo Puan,[∞] Craig T. Morita,[∞] and Eric Oldfield*[,||]

*Center for Biophysics and Computational Biology, University of Illinois at Urbana−Champaign, 607 South Mathews Avenue, Urbana, Illinois 61801, W. M. Keck Center for Comparative and Functional Genomics, University of Illinois at Urbana−Champaign, 1201 West Gregory Drive, Urbana, Illinois 61801, Department of Statistics, University of Illinois at Urbana−Champaign, 725 South Wright Street, Champaign, Illinois 61820, School of Molecular and Cellular Biology, University of Illinois at Urbana−Champaign, 505 South Goodwin Ave, Urbana, Illinois 61801, Division of Rheumatology, Department of Internal Medicine and the Interdisciplinary Group in Immunology, University of Iowa College of Medicine, EMRB 400, Iowa City, Iowa 52242, and Department of Chemistry, University of Illinois at Urbana−Champaign, 600 South Mathews Avenue, Urbana, Illinois 61801*

*Received April 26, 2006*

We screened a library of 117 bisphosphonates for antibacterial activity against *Escherichia coli*. The most potent growth inhibitors where the *N*-[methyl(4-phenylalkyl)]-3-aminopropyl-1-hydroxy-1,1-bisphosphonates, known potent bone resorption inhibitors, and there was a generally good correlation between cell growth inhibition and *E. coli* farnesyl diphosphate synthase (FPPS) inhibition. However, some potent FPPS inhibitors had no activity in cell growth inhibition, and based on the result of Catalyst pharmacophore modeling, this could be attributed to the requirement of a large hydrophobic feature for cellular activity (due most likely to transport). The activity of the most potent compound, *N*-[methyl(4-phenylbutyl)]-3-aminopropyl-1-hydroxy-1,1-bisphosphonate (**13**), was strongly potentiated by the drug fosmidomycin. The transcription profiles for **13** or fosmidomycin alone were different from those found with carbenicillin or ciprofloxacin alone, but there were many similarities between the combination (**13**−fosmidomycin) and carbenicillin or ciprofloxacin, reflecting the more potent bactericidal activity of the drug combination on bacterial growth.

## Introduction

Drug resistance in bacteria is a growing problem and there is a continuous, unmet need for new drug targets and new drugs.[1] The isoprenoid biosynthesis pathway is one such target of interest.[2−6] The central enzyme involved in isoprenoid biosynthesis in all organisms is farnesyl diphosphate synthase (FPPS,[a] EC 2.5.1.10), which condenses dimethylallyl diphosphate (DMAPP, **1**) with isopentenyl diphosphate (IPP, **2**) to form geranyldiphosphate (GPP, **3**), which then condenses with a second IPP molecule to form farnesyl diphosphate (FPP, **4**).

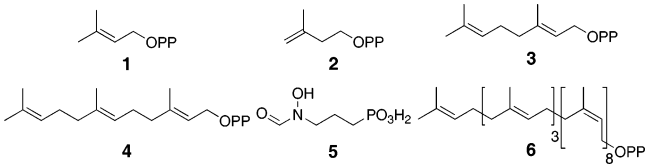


The DMAPP and IPP are made in one of two ways: from the mevalonate pathway or from the non-mevalonate or methylerythritol phosphate (MEP) pathway (Figure 1).[6] In some bacteria, such as *Staphylococcus aureus*, the mevalonate pathway is utilized to make FPP, and several mevalonate pathway enzymes have been proposed to be good targets for drug development, although unfortunately the statins used so extensively to treat hyperlipidemia [by inhibiting the class I hydroxymethylglutaryl coenzyme-A reductase enzyme (HMG-CoA reductase, EC 1.1.1.34)] are essentially inactive against the (class II) bacterial enzymes.[7] However, the alternate MEP pathway[8,9] is present in the majority of pathogenic bacteria and one of its components, deoxyxylulose-5-phosphate reductoisomerase (DXR, EC 1.1.1.267), is potently inhibited[10] by the phosphonate drug fosmidomycin (**5**). Once produced, FPP is converted in bacteria into the $C_{55}$ isoprenoid undecaprenyl diphosphate (UPP, **6**) by UPP synthase (UPPS, EC 2.5.1.31), and UPP is then utilized in the formation of lipid II for cell wall peptidoglycan biosynthesis. UPPS is, consequently, a potentially important drug target.[2−4] FPP is also utilized in the production of ubiquinone and menaquinone, for electron transport. And, in *S. aureus*, FPP is converted to the virulence factor staphyloxanthin, a carotenoid that is thought to be responsible for the resistance of *S. aureus* to the reactive oxygen species produced by the host's immune system.[5] Carotenoids are also present in the group B streptococci[11] and could play a similar role and, although not confirmed, are likely to be produced from FPP. When considered together, there are, therefore, numerous potential isoprenoid biosynthesis pathway enzymes in bacteria that might be targeted, alone or in combination, but to date only fosmidomycin (which inhibits DXR) has been investigated in any detail.[12] In addition to its antibacterial activity, there has recently been considerable interest in fosmidomycin as an antimalarial drug, since it has

* To whom correspondence should be addressed. Phone: (217) 333-3374. Fax: (217) 244-0997. E-mail: eo@chad.scs.uiuc.edu.

[†] Center for Biophysics and Computational Biology, University of Illinois at Urbana−Champaign.

[‡] W. M. Keck Center for Comparative and Functional Genomics, University of Illinois at Urbana−Champaign.

[§] Department of Statistics, University of Illinois at Urbana−Champaign.

[||] Department of Chemistry, University of Illinois at Urbana−Champaign.

[⊥] School of Molecular and Cellular Biology, University of Illinois at Urbana−Champaign.

[∞] University of Iowa.

[a] Abbreviations: methylerythritol phosphate, MEP; farnesyl diphosphate synthase, FPPS; dimethylallyl diphosphate, DMAPP; isopentenyl diphosphate, IPP; geranyldiphosphate, GPP; farnesyl diphosphate, FPP; deoxyxylulose-5-phosphate reductoisomerase, DXR; undecaprenyl diphosphate, UPP; UPP synthase, UPPS; octaprenyl diphosphate synthase, OPPS; hydroxymethylglutaryl coenzyme-A reductase, HMG-CoA reductase; minimum inhibitory concentrations, MIC; minimum bactericidal concentrations, MBC; analysis of variance, ANOVA; false discovery rate, FDR.

10.1021/jm060492b CCC: $33.50 
Published on Web 11/10/2006

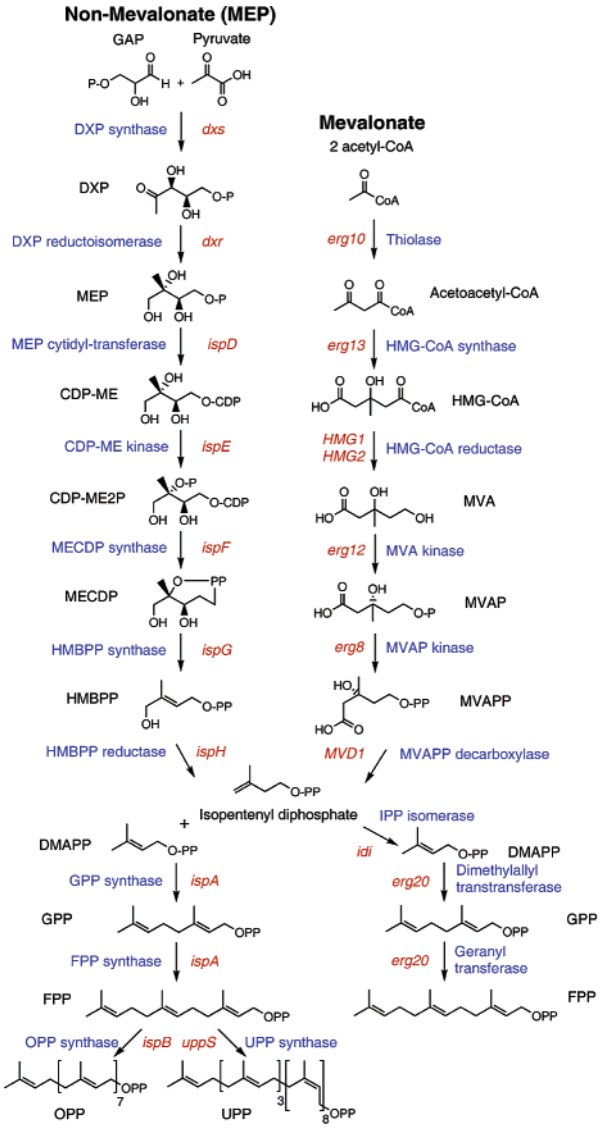


**Figure 1.** Mevalonate, non-mevalonate (MEP), and polyisoprenoid biosynthesis pathways.

been shown that it also inhibits the DXR enzyme in the parasitic protozoan *Plasmodium falciparum*, the organism responsible for the most serious form of malaria. Plus, fosmidomycin has been found to act synergistically with another antibiotic, clindamycin,[13] as well as with artesunate.[14]

The concept of drug synergisms in isoprenoid biosynthesis has also been investigated in other protozoa where, for example, statins synergize with azoles, azoles synergize with a bisphosphonate, azoles synergize with amiodarone, and statins synergize with terbinafine,[15−17] all resulting in greatly reduced synthesis of ergosterol, essential for cell membrane stability in many trypanosomatid parasites. Although quantitative predictions of the extent of synergy are not currently possible, what is clear is that in many cases synergistic interactions are seen when multiple drugs target the same metabolic pathway—even when the actual enzyme targets are quite distant from each other.

Given the central location of FPPS, this enzyme appeared to us to be a good potential target for antimicrobial agents. We therefore screened a library of bisphosphonates (many of which are known, or expected to be, FPPS inhibitors) in *Escherichia coli* and then investigated the synergism of the most potent species with fosmidomycin, the known potent DXR (MEP pathway) inhibitor, as well as two well-known antibiotics, ciprofloxacin and carbenicillin. We then used a microarray analysis to investigate the transcriptional profiles of *E. coli* grown in the presence of these inhibitors (alone and in combination). The results obtained show that the bisphosphonate−fosmidomycin combination can be highly synergistic (fractional inhibitory concentration index, FICI = 0.15), opening up new possibilities for antibacterial combination therapy targeting the isoprenoid biosynthesis pathway. In addition, we carried out structure−activity relationship investigations for cell growth as well as FPPS inhibition using pharmacophore modeling, as a prelude to the future development of even more potent bisphosphonates, for use in combination therapy.

## Materials and Methods

**Experimental Section. Reagents.** Fosmidomycin was purchased from Molecular Probes (Eugene, OR), carbenicillin from Fisher Biotech (Fair Lawn, NJ), and ciprofloxacin hydrochloride from ICN Biomedical Inc. (Aurora, OH). Antibiotic sensitivity disks (chloramphenicol, kanamycin, novobiocin, tetracycline, streptomycin, and neomycin) were purchased from Nebraska Scientific (Omaha, NE). Other reagents were from Sigma-Aldrich (St. Louis, MO). The bisphosphonates tested were from an existing library, reported previously.[18−25]

**Antimicrobial Susceptibility Screening.** We first tested 117 bisphosphonates (**7**−**123**; Supporting Information Table S1), fosmidomycin, and six control antibiotics (chloramphenicol, kanamycin, novobiocin, tetracycline, streptomycin, and neomycin) for activity against *E. coli* W3110 using a standard Kirby−Bauer disc diffusion method.[26] Four or five colonies picked from an overnight culture were inoculated into 10 mL of Luria−Bertani (LB) broth medium and incubated at 37 °C for 2 h, with agitation (200 rpm). The culture was spread over the surface of Mueller−Hinton (MH) agar plates. Then, 6-mm sterile discs (Nebraska Scientific) were placed on the plate, and 10 $\mu$L of a 20 mM bisphosphonate solution was added. Additional screening was carried out with fosmidomycin (10 $\mu$L of a 20 mM solution) and with the antibiotic sensitivity discs containing 30 $\mu$g of chloramphenicol, kanamycin, novobiocin, tetracycline, streptomycin, and neomycin as controls. Plates were incubated overnight at 37 °C and then the diameter of the zone of growth inhibition was measured. We then investigated the most active species using an *E. coli* W3110 transformant containing a TMV19 plasmid, consisting of five enzymes of the mevalonate pathway (from HMG-CoA synthase to diphosphomevalonate decarboxylase).[27] In this transformant, growth inhibition by FPPS inhibition is not expected to be rescued by mevalonate (1 mg/mL in the medium), while growth inhibition by blocking the MEP pathway (e.g., by fosmidomycin) is rescued by mevalonate, since the five-gene cluster provides an alternate route to IPP synthesis.

**$IC_{50}$ Determinations.** We determined the $IC_{50}$ value for the most active bisphosphonates found in the Kirby−Bauer assay, together with the $IC_{50}$ values for fosmidomycin, ciprofloxacin, and carbenicillin, in *E. coli* K12 (ATCC, Manassas, VA), by using a broth microdilution method.[28] For each compound, two independent experiments were performed and the $IC_{50}$ values found were averaged. An overnight culture of *E. coli* K12 (37 °C, 200 rpm agitation) was diluted 50-fold into LB broth medium and incubated to an $OD_{600}$ of ~0.4. The culture was then diluted 500-fold into LB broth medium. Then 90 $\mu$L of this *E. coli* inoculum was inoculated into a 96-well flat bottom culture plate (Corning Inc., Corning, NY) containing 10 $\mu$L of the test compounds, previously half-log serial diluted in LB broth medium. The concentration range was 0.316 mM to 1 nM. Plates were incubated for 3 h at 37 °C (midexponential phase). An MTT [(3-(4,5-dimethylthiazol-2-yl)-2,5-diphenyltetrazolium bromide] cell proliferation assay (ATCC) was then carried out, as described,[29] to obtain bacterial viability dose−response curves. A nonlinear regression analysis was carried out on the data obtained by using GraphPad PRISM version 4.00 for Windows (GraphPad Software Inc., San Diego, CA,

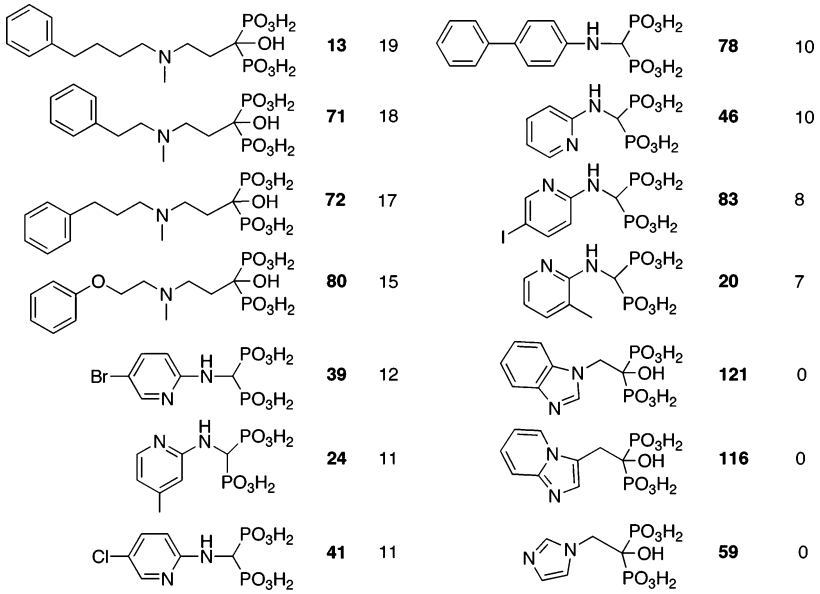


**Figure 2.** Structures of selected compounds in *E. coli* W3110 growth inhibition (Kirby−Bauer values, in mm, not bolded). Results for all compounds investigated are shown in the Supporting Information (Table S1).

www.graphpad.com). The experimental results were then fit to the rectangular hyperbolic function

$$I = \frac{I_{max} C}{IC_{50} + C} \quad (1)$$

where $I$ is the percent inhibition, $I_{max} = 100\%$ inhibition, $C$ is the concentration of the inhibitor, and $IC_{50}$ is the concentration for 50% growth inhibition.

***E. coli* FPPS Inhibition.** The *E. coli* FPPS assays were carried out using 96-well plates with 200 $\mu$L reaction mixture in each well. The condensation of GPP and IPP was monitored by a continuous spectrophotometric assay[30] for phosphate releasing enzymes. The reaction buffer contained 50 mM Tris-HCl, 1 mM $MgCl_2$, at pH 7.4. The compounds investigated were preincubated with *E. coli* FPPS for 30 min at 4 °C. The $IC_{50}$ values were obtained by fitting the inhibition data to the dose−response curve in Origin 6.1 (OriginLab Corp., Northampton, MA, www.OriginLab.com).

**Checkerboard Assays.** We investigated the possibility of synergistic interactions between the most potent bisphosphonate found (**13**, Figure 2) and fosmidomycin in *E. coli* K12, in addition to five other, two-drug combinations (**13**−carbenicillin, **13**−ciprofloxacin, fosmidomycin−carbenicillin, fosmidomycin−ciprofloxacin, and carbenicillin−ciprofloxacin) using a 2-fold dilution checkerboard assay method with concentration values from 1/16 to 4 times the $IC_{50}$ value of each drug,[31] plus no-drug controls. The $IC_{50}$ values were determined for each combination of drugs in two independent experiments by averaging the values found. The fractional inhibitory concentration index (FICI) was then calculated by using eq 2

$$FICI = FIC_A + FIC_B = IC_{50}(AB)/IC_{50}(A) + IC_{50}(BA)/IC_{50}(B) \quad (2)$$

where, $FIC_A$, $FIC_B$ are the fractional inhibitory concentrations of drugs A and B, $IC_{50}(A)$ and $IC_{50}(B)$ are the $IC_{50}$ values of drugs A and B acting alone, and $IC_{50}(AB)$ and $IC_{50}(BA)$ are the $IC_{50}$ values of the most effective combination of drug A or B in the presence of drug B or A.[31,32] Using this method, FICI values of $<0.5$ represent synergism, $>0.5$ and $<1.0$ represent additivism, $>1$ and $<2$ represent an indifferent effect, and $\geq 2$ represents drug antagonism.[33] In addition, we evaluated Loewe additivity difference response surfaces and $IC_{50}$ isobolograms using the methods of Suhnel[34] and Berenbaum,[35] respectively.

**Susceptibility Test.** The susceptibility of *E. coli* K12 to **13**, fosmidomycin, **13**−fosmidomycin, carbenicillin, and ciprofloxacin (positive control) were deduced from the minimum inhibitory concentrations (MIC) and the minimum bactericidal concentrations (MBC) using a broth microdilution technique (NCCLS M7-A5[28]). MIC values were determined using a 5 $\mu$L inoculum of $10^5$ cfu/mL in 96-well flat bottom plates containing 100 $\mu$L of the test compounds, previously 2-fold serial diluted in LB broth medium. Plates were incubated at 37 °C for 24 h. The MICs represent the lowest concentrations of drug that inhibit bacterial growth. MBC values were determined by plating 10 $\mu$L of each microtiter well without visible growth onto drug-free medium (LB agar) for an O/N incubation. The MBCs were the first dilution at which no growth was observed.

**Culture Conditions for DNA Microarray Experiments.** Three independent sets of experiments were carried out, in triplicate. *E. coli* K12 was grown under aerobic conditions (37 °C, 200 rpm agitation in LB broth medium). An O/N culture was diluted 500-fold into LB broth medium (in triplicate) and incubated to early exponential phase ($OD_{600} \sim 0.2$). Each culture was then split into 15-mL aliquots and one aliquot from each culture was left untreated (control), while the other five aliquots were treated with previously determined ($IC_{50}$) amounts of **13**, fosmidomycin, **13**−fosmidomycin, carbenicillin, or ciprofloxacin. Incubation of all samples (three 15 mL cultures for each treatment, including a control culture) was then continued under the same conditions for 1 h (midexponential phase), prior to RNA extraction.

**RNA Isolation.** Cells were harvested and resuspended in 1 mL of RNA STAT-60 (Tel-Test Inc, Friendswood, TX) for total RNA extraction. All subsequent purification steps were carried out according to the RNA STAT-60 reagent manual.[36] The three RNA samples obtained per treatment were then pooled before microarray hybridization, in order to minimize any possible differences between cultures.

**High-Density Oligonucleotide Microarray Analysis.** Sixteen RNA samples were used for DNA microarray analysis: three samples each from the control cultures or from cultures treated with **13**, fosmidomycin, or the combination of **13**−fosmidomycin and two samples each from cultures treated with carbenicillin or ciprofloxacin. Affymetrix GeneChip antisense *E. coli* K12 genome arrays (Affymetrix Inc., Santa Clara, CA) were used to analyze the complete *E. coli* transcriptome. cDNA synthesis, fragmentation, and labeling were carried out as described in the Affymetrix GeneChip *E. coli* Antisense Genome Array Technical Manual, by Genome Exploration Inc. (Memphis, TN). Each labeled sample was

hybridized to one GeneChip. After washing and staining, GeneChips were scanned at 570 nm and 3 $\mu$m pixel resolution in an Affymetrix GeneChip scanner and probe raw intensity files were generated for analysis.[37]

**Statistical Analysis.** To reduce global systematic variations in the data across arrays caused by inconsistencies in labeling and/or loading ("nonbiological differences"), invariant-set normalization was performed on the raw intensity data using the DNA-Chip Analyzer algorithm (dChip, http://www.dchip.org). This normalization protocol iteratively selects probes from presumably nondifferentially expressed genes.[38] To identify significant changes in gene expression under different drug treatments, analysis of variance (ANOVA) was performed one gene at a time in SAS (SAS Institute Inc., Cary, NC). On the basis of the approach reported by Chu et al.,[39] the ANOVA model for one gene is given by

$$\log_2(\mathrm{PM}_{ijk}) = \mathrm{treatment}_i + \mathrm{probe}_j + \mathrm{array}_k(\mathrm{treatment}_i) + e_{ijk} \quad (3)$$

where, $i = 1-6$; $j = 1 - J$; and $k = 1 - K$; $J$ is the number of replicates for each treatment ($J = 2$ or 3), and $K$ is the number of probes for the gene being analyzed ($K = 14$ or 15). In the ANOVA model, $\log_2(\mathrm{PM}_{ijk})$ is the logarithm (base 2) transformed perfect-match intensity measurement for the $i$th treatment in the $j$th replicate at the $k$th probe, treatment and probe are the treatment and probe main effects, respectively, array (treatment) is the (fixed) array nested within the treatment effect, and $e_{ijk}$ is a random error, assumed to be independent normal variables with zero mean and common variance. The false discovery rate (FDR) was used for multiple test adjustment in a given comparison. A gene was regarded as being a significant gene if it showed statistically significant change in expression as defined by an FDR adjusted $p$-value (FDR-$p$) of less than 0.05.

**Clustering.** Genes that showed significant changes in expression (FDR-$p < 0.05$) with at least one treatment when compared to the control were used to form a data matrix. In this matrix, rows are genes, columns are drug treatments, and the values are the estimated mean signal intensity of probe set intensities from the normalized probe intensities. The data matrix was imported into GeneSpring software (Agilent Technology, Palo Alto, CA). The signal intensity of each gene was then transformed into expression ratios to the control (relative gene expression) using "per gene" normalization. Hierarchical clustering analysis was performed using the standard correlation as a similarity measure across drug treatments. A minimum distance of 0.001 and a correlation difference among drugs, defined by a separation ratio of 0.5 (the default value from the software), were used.

**Computational Methods.** Pharmacophore (common feature) models were generated in Catalyst 4.11 (Accelrys, Inc., San Diego, CA) using the HypoGen, HypoRefine, and HipHop modules. Conformers of each molecule were generated within Catalyst. Each dataset included up to 256 conformers of each molecule within a 20 kcal/mol range of the minimum energy conformer. Two negative ionizable, two hydrophobic, and one positive charge feature were selected from the feature dictionary, for potential mapping. Default values were used for all parameters. The top five common feature hypotheses were reported, and final selection was based on rank.

## Results and Discussion

**Growth Inhibition Results.** We first carried out a Kirby–Bauer screen of 117 bisphosphonates against *E. coli* W3110 as well as against an *E. coli* W3110 transformed with the expression plasmid pTMV19 (*E. coli*-pTMV19) containing the initial enzymes of the mevalonate pathway (from *Streptomyces* sp. strain CL190): HMG-CoA synthase, HMG-CoA reductase, mevalonate kinase, phosphomevalonate kinase, and diphosphomevalonate decarboxylase.[27,40] The presence of these enzymes allows the transformant to grow, even if the MEP pathway was blocked, e.g., by fosmidomycin, as long as sufficient mevalonate is present to permit isoprenoid biosynthesis through the mevalonate pathway. The growth inhibition results (in mm) are given in the Supporting Information (Table S1) for all compounds versus *E. coli* W3110 and for the most active compounds against the transformant (in the absence and presence of mevalonate).

**Table 1.** $IC_{50}$ Values Determined for **13** and Fosmidomycin in *E. coli* K12 (Wild Type), *E. coli* Overexpressing *T. brucei* FPPS (*E. coli*-FPPS$^{++}$), and *E. coli* Overexpressing *E. coli* DXR (*E. coli*-DXR$^{++}$)

| | $IC_{50}$ ($\mu$M) | | |
|---|---|---|---|
| compd | *E. coli* K12 | *E. coli*-FPPS$^{++}$ | *E. coli*-DXR$^{++}$ |
| **13** | 33 | 444 | 245 |
| fosmidomycin | 0.22 | 0.20 | 1853 |

What can immediately be seen from the results in Table S1 is that the vast majority of the bisphosphonates investigated have little or no activity in inhibiting *E. coli* W3110 growth. However, a minority of compounds have activity and the structures of a selection of these are shown in Figure 2, rank ordered in terms of decreasing activity. Interestingly, all of the most active compounds are known potent FPPS inhibitors and/or bone resorption[41] drugs (e.g., **13**, **71**, **72**, **80**), and on the basis of the mevalonate rescue experiments with the transformant, these compounds target FPPS in *E. coli* as well. Surprisingly, however, other highly potent bone resorption drugs such as minodronate (**116**, Figure 2) and zoledronate (**59**, Figure 2) have no activity against *E. coli* growth, suggesting the need for a more in depth investigation of structure–activity relationships.

In previous work, we used pharmacophore modeling and 3D-QSAR (three-dimensional quantitative structure–activity relationship) methods to investigate the structural features of these and a variety of other compounds active in bone resorption, finding that the presence of two negative ionizable groups, a positive charge center, and at least one aromatic feature was necessary for high activity,[42] and a similar set of features was also observed in FPPS inhibition.[21] Here, however, we find that other known, potent FPPS inhibitors such as risedronate (**8**) and zoledronate (**59**) have no measurable activity against *E. coli*

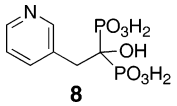


**8**

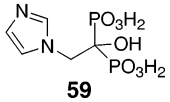


**59**

W3110 cell growth. That is, only the long, phenylalkyl species have significant activity against *E. coli* W3110. This might be attributable to inherent differences in activity between the human and *E. coli* enzymes; to the possibility that, e.g., **13**, **71**, and **72** inhibit another, unknown target in *E. coli*; or to the poorer cell permeability of the smaller pyridinium and imidazolium molecules as compared to the phenylalkyl bisphosphonates. Inhibition by **13** of enzymes of the MEP pathway is ruled out by the experiments on the *E. coli*-pTMV19 transformant, which failed to grow in the presence of mevalonate. Moreover, **13** has no activity (at 200 $\mu$M) against either an expressed *E. coli* octaprenyl diphosphate synthase (OPPS), an expressed *E. coli* UPPS, or against an expressed *E. coli* DXR (unpublished results). To test the working hypothesis that FPPS is the target for **13** in *E. coli*, we therefore next determined the $IC_{50}$ value for *E. coli* K12 growth inhibition by **13** in a broth microdilution experiment and then compared this result with that obtained for *E. coli* BL21 (DE3) overexpressing *Trypanosoma brucei* FPPS (ref 18 contains the plasmid description). We found an $IC_{50}$ value of 33 $\mu$M for **13** against *E. coli* K12, but this value increased by a factor of ~13, to 444 $\mu$M, in the overexpressing strain (Table 1). That is, far more **13** was required to inhibit the *E. coli* strain overexpressing FPPS. These results all strongly

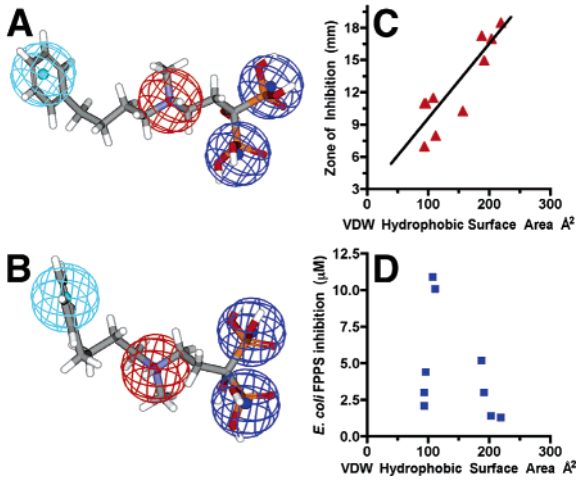


**Figure 3.** Catalyst common feature hypothesis: (A) for *E. coli* growth inhibition superimposed on the most active cell growth inhibitor; (B) for *E. coli* FPPS inhibition, superimposed on the most active compound **13**; both pharmacophores contain two negative ionizable groups (dark blue), a hydrophobic feature (cyan) and a positive charge feature (red); (C) correlation between van der Waals hydrophobic surface area and *E. coli* growth inhibition ($r^2 = 0.78$); and (D) correlation between hydrophobic surface area and *E. coli* FPPS inhibition.

support the idea of an FPPS target for **13** in *E. coli*, and the efficacy of the most potent *E. coli* growth inhibitors appears to be related to the presence of their large, hydrophobic side chains. Compounds **41** and **39** are less active than **13** and **72**, and as with the most potent inhibitors, they also inhibit growth in the transformant in the presence of mevalonate (Supporting Information, Table S1) and are known to be FPPS inhibitors (of the *Leishmania major* enzyme), with $K_i$ values of 23 nM (**41**) and 140 nM (**39**),[21] making once again FPPS a likely target for their action. However, while similar activity is found for **112** and **57**, these compounds are not likely to act via FPPS inhibition, based on the observation that mevalonate rescues transformant growth inhibition by these compounds (Supporting Information, Table S1).

Clearly, these results are somewhat surprising in that potent bone resorption bisphosphonate drugs such as risedronate (**8**), minodronate (**116**), and zoledronate (**59**) have no activity versus *E. coli*, while the longer chain phenylalkyl bisphosphonates (**13**, **71**, **72**) are the most active species, both in the zone inhibition results and in suspension culture (where zoledronate and risedronate are again inactive). To investigate this topic in more detail, we used a common feature hypothesis approach to try to clarify which features contribute most to cell and enzyme activity.

We used growth inhibition data from the 11 compounds, shown in Figure 2, which act via FPPS inhibition (based on the mevalonate rescue experiments with the transformant, Supporting Information Table S1), to construct a series of common feature models. We chose as an initial model a pharmacophore containing the features observed previously in FPPS inhibition: two negative ionizable features (corresponding to the two phosphonate groups), one hydrophobic feature (mapping in all compounds), and a positive charge feature. The resulting common feature hypothesis shown in Figure 3A is clearly quite similar to previously published FPPS pharmacophores[42] for bone resorption by **13** and related compounds.

We then investigated pharmacophores for *E. coli* FPPS inhibition. Since we were puzzled by the lack of activity of some potent bisphosphonates in *E. coli* growth inhibition, we chose to investigate FPPS inhibition by three known potent

**Table 2.** Most Potent *E. coli* FPPS Inhibitors Used To Construct the Common Feature Hypothesis, Shown in Order of Decreasing Potency

| compd | $IC_{50}$ ($\mu$M) | compd | $IC_{50}$ ($\mu$M) |
|---|---|---|---|
| **121** | 0.7 | **13** | 1.3 |
| **116** | 1.1 | **72** | 1.4 |
| **59** | 1.1 | **24** | 2.1 |

FPPS inhibitors (zoledronate, **59**; minodronate, **116**; and a benzimidazole species, **121**; Figure 2) that were inactive in cell growth inhibition, in addition to three very active species (**13**, **71**, and **72**; Figure 2). The experimental $IC_{50}$s are given in Table 2. As can be seen from these results, the lack of effect of **59**, **116**, and **121** on *E. coli* cell growth is not due to the lack of FPPS inhibition, since all three are potent FPPS inhibitors, and are actually slightly more potent than the phenylethyl bisphosphonates **13**, **71**, and **72**. A common feature model for *E. coli* FPPS inhibition is shown in Figure 3B. The lack of the distal hydrophobic feature (in, e.g., zoledronate, **59**) accounts for the lack of cellular activity of these and other known potent FPPS inhibitors in *E. coli* cell growth inhibition. Of course, this feature is not critical for FPPS inhibition, since zoledronate (**59**) is in fact a potent FPPS inhibitor. The high activity of zoledronate and related systems against FPPS can, however, also be achieved due to the presence of a more proximal aromatic ring feature,[42] so either the distal hydrophobic or the more proximal aromatic ring feature can contribute to FPPS inhibition activity.[42] However, the presence of the distal phenyl alkyl moiety is critical for *E. coli* cell growth inhibition (Figure 3A). The importance of having a large hydrophobic feature for *E. coli* growth inhibition is also clearly seen in Figure 3C, in which there is a good correlation ($r^2 = 0.78$) between the van der Waals hydrophobic surface area and the zone of inhibition result, while this correlation is not seen in the FPPS inhibition results ($r^2 = 0.22$, Figure 3D), again suggesting the important role of transport in the *E. coli* cell growth inhibition results.

With fosmidomycin, the $IC_{50}$ for growth inhibition in *E. coli* K12 was 0.22 $\mu$M (Table 1), essentially the same as that in the FPPS overexpressing strains ($IC_{50} = 0.20$ $\mu$M, Table 1), but as expected this value increased considerably in *E. coli* M15 overexpressing *E. coli* DXR (~2 mM, Table 1, ref 45 contains the plasmid description). Interestingly, the $IC_{50}$ for inhibition by **13** in the DXR overexpressing strain ($IC_{50} = 245$ $\mu$M) was also higher than the value found in the wild type strain, due presumably in this case to increased flux through the isoprenoid biosynthesis pathway due to overexpression of DXR, since **13** has essentially no activity against an expressed *E. coli* DXR (data not shown).

Given these results, we next sought to improve efficacy by testing the idea that **13** might act synergistically with fosmidomycin (which inhibits the DXR enzyme, upstream of FPPS), since both are involved in isoprenoid biosynthesis. While we thought that such synergy might be seen, in another cases,[43] two isoprenoid biosynthesis pathway inhibitors lacked any synergy,[43] necessitating an experimental investigation of this topic. We also tested two other, known antibacterial drugs, ciprofloxacin and carbenicillin (having $IC_{50}$ values of 32 nM and 5.8 $\mu$M, respectively), for possible synergistic effects with **13** and fosmidomycin. And for completeness, we investigated all six possible two-drug combinations: **13**−fosmidomycin, **13**−carbenicillin, **13**−ciprofloxacin, fosmidomycin−carbenicillin, fosmidomycin−ciprofloxacin, and carbenicillin−ciprofloxacin. The combined effects of these compounds were mathematically represented via the FICI values. The combination **13**−fosmidomycin was found to be highly synergistic (FICI = 0.15)

**Table 3.** Fractional Inhibitory Concentration Indices (FICI) of Drug Combinations Investigated

| combination | FICI | interaction |
|---|---|---|
| **13**−fosmidomycin | 0.15 | synergism |
| **13**−carbenicillin | 1.58 | indifference |
| **13**−ciprofloxacin | 0.89 | additivism |
| fosmidomycin−carbenicillin | 1.21 | indifference |
| fosmidomycin−ciprofloxacin | 1.96 | indifference |
| carbenicillin−ciprofloxacin | 2.72 | antagonism |

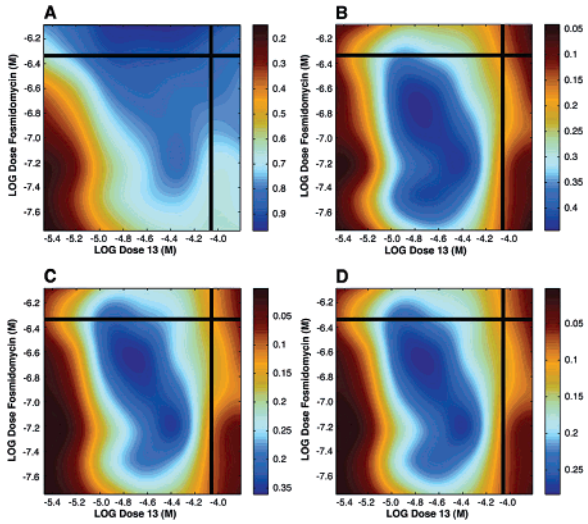


**Figure 4.** Diagrams showing effects of the combination **13**−fosmidomycin on *E. coli* K12 cell growth. (A) Contour surface for the fractional effect of the drug combination. The dark lines indicate single agent $IC_{50}$s, and the blue regions indicate high fractional effect. Notice the elevated fractional effect achieved by the **13**−fosmidomycin combination below the single agent $IC_{50}$. (B) Contour plot of Loewe additivity difference response surface. *Z*-axis values greater than zero are indicative of Loewe synergy. In its most synergistic concentration regime, the **13**−fosmidomycin combination exhibits a fractional effect approximately 40% greater than that calculated for zero interaction between the two agents. (C) Surface showing product of A and B (experimental effect x excess over Loewe additivity). (D) Surface showing product of surface C divided by total drug dose.

(Table 3). The other combinations tested acted in either an indifferent (**13**−carbenicillin; fosmidomycin−carbenicillin, and fosmidomycin−ciprofloxacin), additive (**13**−ciprofloxacin), or antagonistic (carbenicillin−ciprofloxacin) manner (Table 3). These results were confirmed by using Loewe additivity difference response surfaces and $IC_{50}$ isobolograms, as shown for **13**−fosmidomycin in Figure 4 and in the Supporting Information (Figure S6A). The **13**−fosmidomycin combination exhibited Loewe additivity difference response values of up to 40% greater than that calculated for zero interaction between the two compounds (Figure 4B). Figure 4C shows a contour plot of Loewe additivity difference response values multiplied by fractional effect values for all experimental concentrations. Dark blue here is indicative of Loewe synergy optimized for highest fractional effect. Figure 4D shows a contour plot of Loewe additivity difference response values multiplied by fractional effect values and divided by a total dosage value for all experimental concentrations. Dark blue here is indicative of Loewe synergy optimized for highest fractional effect and lowest combination dosage from which it can again be seen that there are strongly synergistic regions. These results were confirmed by the $IC_{50}$ isobologram, which was distinctly concave-up and had a CI value of 0.23 at its inflection point (Supporting Information, Figure S6A), consistent with the FICI result shown in Table 3. Results for the other five combinations are shown in Figures S1−S6 in the Supporting Information. Of all the combinations investigated, only **13**−fosmidomycin showed a clearly synergistic interaction.

**Table 4.** MIC and MBC Values in *E. coli* K12

| compd | MIC ($\mu$M) | MBC ($\mu$M) | MIC/MBC |
|---|---|---|---|
| **13** | 156 | 1250 | 0.13 |
| fosmidomycin | 312 | 2500 | 0.13 |
| **13**−fosmidomycin | 312 | 625 | 0.50 |
| carbenicillin | 20 | 20 | 1 |
| ciprofloxacin | 0.038 | 0.076 | 0.50 |

**MIC/MBC Results.** We next investigated the MIC and MBC values for **13**, fosmidomycin, their combination, and, by way of a control, carbenicillin and ciprofloxacin. For bactericidal activity, MIC ∼ MBC, while for bacteriostatic activity, MIC < MBC. The results obtained are shown in Table 4 and indicated that both **13** and fosmidomycin, under the growth conditions used, are bacteriostatic. In contrast, the combination has an MIC/MBC ratio of ∼2 and is therefore in the range expected for bactericidal activity as seen, e.g., with carbenicillin (MIC/MBC = 1, Table 4). These results are consistent with the potent synergistic activity seen with the **13**−fosmidomycin combination and with the microarray results described below.

**Changes in Gene Expression Patterns in Response to Drugs.** In order to try to better understand the origins of the synergistic effects described above, we next examined the effects of **13**, fosmidomycin, carbenicillin, ciprofloxacin, as well as the combination **13**−fosmidomycin on gene transcription profiles in *E. coli* K12, using a microarray analysis. Ciprofloxacin and carbenicillin were employed as positive controls. Three independent RNA samples were obtained for each experimental condition and were hybridized to Affymetrix GeneChips antisense *E. coli* K12 genome arrays, except in the case of carbenicillin and ciprofloxacin, where only two RNA samples were hybridized. The control results obtained with carbenicillin and ciprofloxacin were in good accord with results described previously.[44]

The total number of significant genes (FDR-$p$ < 0.05) was calculated from the union of genes that showed significant changes in at least one of the treatments (**13**, fosmidomycin, **13**−fosmidomycin, carbenicillin, and ciprofloxacin), and the percentage of genes having significant (FDR-$p$ < 0.05) changes in expression (up- or down-regulated) was calculated with respect to the total number of these significant genes. Out of 4345 open reading frames (ORF) contained in the Affymetrix GeneChip antisense *E. coli* K12 genome array, we found that a total of 3954 genes were significantly affected by at least one of the five treatments, when compared to the controls.

Figure 5 shows Venn diagrams representing the relationships between the effects of **13**, fosmidomycin, and their combination (Figure 5A,B); the relationship between the effects of **13**, carbenicillin, and ciprofloxacin (Figure 5C,D); and the relationship between the effects of the combination (**13**−fosmidomycin), carbenicillin, and ciprofloxacin (Figure 5E,F). Compound **13** and fosmidomycin acting alone were found to have similar effects on gene transcription. For example, **13** up-regulated 28.2% (2.4 + 17.5 + 5.3 + 3.0 = 28.2%) or 1116 genes, while fosmidomycin up-regulated 1219 (30.8%) genes, there being 17.5% common genes up-regulated (Figure 5A). Likewise, there were 19.4% of the total significant genes commonly down-regulated by both treatments, respectively (Figure 5B). These values are significantly larger than the percentage of genes that were only affected by **13** (2.4% up-regulated and 3.5% down-

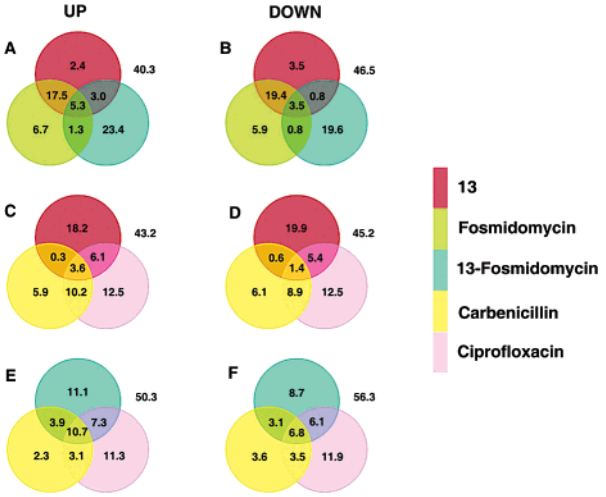


**Figure 5.** Venn diagrams of the effects on *E. coli* K12 gene expression of **13**, fosmidomycin, the combination **13**−fosmidomycin, carbenicillin, and ciprofloxacin. Each circle represents the percentage of genes with significant changes in expression compared to the total number of significant genes. The numbers on the right of each Venn diagram represent the percentage of the significant genes that were not affected by any of the drugs being compared. The overlapping regions represent common genes affected by two (or three) of the treatments. Genes with significant increases in expression are represented on the left (UP); those with significant decreases in expression, on the right (DOWN). (A) **13** versus fosmidomycin versus the combination (**13**−fosmidomycin), up-regulated; (B) **13** versus fosmidomycin versus the combination (**13**−fosmidomycin), down-regulated; (C) **13** versus carbenicillin versus ciprofloxacin, up-regulated; (D) **13** versus carbenicillin versus ciprofloxacin, down-regulated; (E) **13**−fosmidomycin combination versus carbenicillin versus ciprofloxacin, up-regulated; (F) **13**−fosmidomycin combination versus carbenicillin versus ciprofloxacin, down-regulated.

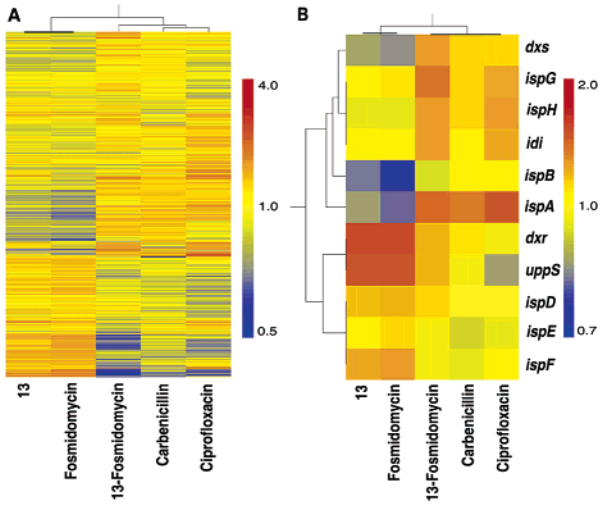


**Figure 6.** Dendrogram showing a hierarchical cluster analysis of *E. coli* K12 responses to **13**, fosmidomycin, the combination **13**−fosmidomycin, carbenicillin, and ciprofloxacin. (A) Genes that significantly changed their expression relative to the control in at least one of the treatments. (B) Eleven genes from the isoprenoid biosynthesis pathway. The scale represents relative gene expression ratios relative to the control (no drug treatment). Relative increases in mRNA levels are shown in red, decreases in blue, and no change in yellow. Both data sets show considerable similarities between **13** and fosmidomycin treatments, while the combination treatment (**13**−fosmidomycin) more closely resembles the effects seen with ciprofloxacin and carbenicillin.

regulated) or fosmidomycin (6.7% up-regulated and 5.9% down-regulated) alone, suggesting similarities in their mechanism of action.

As expected, the genes affected by **13** were very different from those affected by carbenicillin or ciprofloxacin (Figure 5C,D), indicating that **13** targeted a different pathway from the ones affected by the other two drugs. Few genes were found to be commonly regulated by **13** and carbenicillin (0.3% up-regulated and 0.6% down-regulated) or by **13** and ciprofloxacin (6.1% up-regulated and 5.4% down-regulated).

On the other hand, we did not find a high number of genes commonly regulated between **13** and fosmidomycin acting alone, compared to their combination (Figure 5A,B). The combination **13**−fosmidomycin only up-regulated 3.0% of total significant genes in common with **13** and 1.3% with fosmidomycin, while the combination up-regulated by itself a total of 23.4% of genes (Figure 5A). Moreover, only 0.8% of genes were commonly down-regulated by the combination and **13** or by the combination and fosmidomycin (Figure 5B). In sharp contrast, there were considerable similarities between the combination treatment (**13**−fosmidomycin) and the effects of carbenicillin or the most potent inhibitor, ciprofloxacin (Figure 5E,F), clearly a very different pattern to that seen in Figure 5A,B for the drugs acting alone. These results indicate the potent effect on gene transcription of the combination **13**−fosmidomycin when compared to **13** or fosmidomycin when acting alone, consistent with the strong synergism seen in the combination **13**−fosmidomycin (Figure 4, Table 3). But which genes are regulated?

**Cluster Analysis of *E. coli* K12 Transcriptome in Response to Drugs.** To answer this question, we computed the ratio between the mean signal intensity values for each gene and its control on each treatment, in order to determine the relative changes in gene expression. Genes that showed significant changes (FDR-$p < 0.05$) in expression in at least one drug treatment were then used in a hierarchical clustering analysis, to explore similarities in expression profiles between the drugs. The dendogram shown in Figure 6A represents the correlation (from left to right) between *E. coli* K12 responses to compounds **13**, fosmidomycin, the combination **13**−fosmidomycin, carbenicillin, and ciprofloxacin. From these results it can immediately be seen that the relative gene expression patterns of **13** and fosmidomycin acting alone are very similar, but both patterns are quite different from the patterns seen with their combination, with carbenicillin, or with ciprofloxacin (Figure 6A). Moreover, the results found with the **13**−fosmidomycin combination appear similar to those seen with ciprofloxacin. Three main clusters were observed: **13** and fosmidomycin acting alone form the most stringent cluster and carbenicillin and ciprofloxacin the least stringent one, while the combination **13**−fosmidomycin forms an independent cluster that is, however, closely linked to the carbenicillin−ciprofloxacin cluster, reflecting at least qualitatively the potent bactericidal activity of the combination.

To further analyze the apparent similarities in effects on gene transcription with **13** and fosmidomycin, we carried out a hierarchical cluster analysis of the relative gene expression values of all of the isoprenoid (MEP/polyisoprenoid) biosynthesis genes (*dxs*, *dxr*, *ispD*, *ispE*, *ispF*, *ispG*, *ispH*, *idi*, *ispA*, *ispB*, *uppS*) under each of the five different drug treatments. The chemical structures of the intermediates, the genes, and the enzyme names are shown in Figure 1.

Nine of the eleven isoprenoid biosynthesis genes showed significant changes in expression in at least one treatment, the exceptions being *ispD* and *ispE* (Supporting Information, Table S4), and there were two main clusters found across drug treatments (the vertical dendogram of Figure 6B). Compound **13** and fosmidomycin exhibit high similarity in relative gene expression pattern and form the first cluster, while carbenicillin, ciprofloxacin, and the combination **13**−fosmidomycin form the

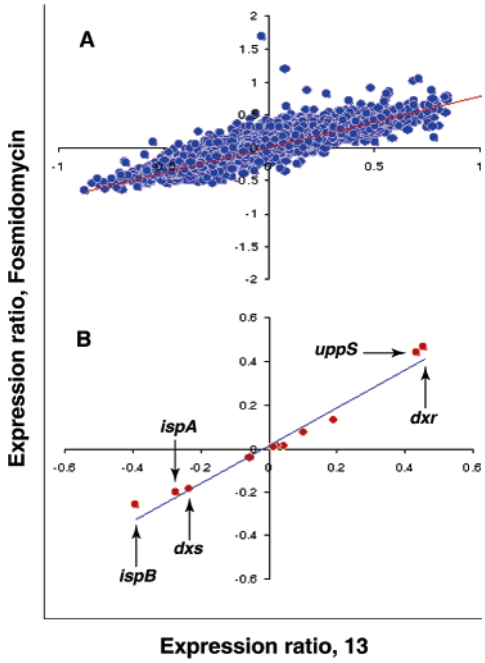


**Figure 7.** Relative increases and decreases in *E. coli* K12 gene expression levels on treatment with fosmidomycin and compound **13**. Each point represents the $\log_2$ expression ratio (to control) of one gene. The expression ratio is calculated for each gene from its estimated mean signal intensity determined for one treatment, divided by the estimated mean signal intensity of that gene in untreated cells. (A) The 4345 ORFs contained in the Affymetrix GeneChip antisense *E. coli* genome array ($R^2 = 0.777$). (B) The eleven isoprenoid biosynthesis pathway genes ($R^2 = 0.972$, $p < 2.54 \times 10^{-8}$).

second cluster. Inspecting the relationship among the genes based on relative gene expression patterns across drug treatments (the horizontal dendrogram on the left of Figure 6B), there are a total of six clusters. One cluster is formed containing DXR (*dxr*) and UPPS (*uppS*) genes, which are uniquely up-regulated by both **13** and fosmidomycin. Another three independent clusters are formed by genes encoding DXP (*dxs*), FPP (*ispA*), and OPP (*ispB*) synthases, which are all clearly down-regulated by both **13** and fosmidomycin. However, *dxs* is up-regulated by the combination **13**−fosmidomycin, and *ispA* is commonly up-regulated by the combination **13**−fosmidomycin, carbenicillin, and ciprofloxacin. The gene *ispF*, which was up-regulated only by fosmidomycin, forms another cluster with the two unchanged genes (*ispD* and *ispE*). The rest of the genes (*ispG*, *ispH*, and *idi*), which form the last cluster, had no significant changes in their expression by either **13** or fosmidomycin treatments but were up-regulated by the combination **13**−fosmidomycin, and *ispH* was also up-regulated by carbenicillin (Figure 6B, Supporting Information, Table S4).

To further investigate the similarities observed in the gene transcription profiles in *E. coli* K12 treated with **13** and with fosmidomycin, the $\log_2$ expression ratio (to control) data sets of fosmidomycin and **13** were compared (Figure 7A,B). The results for all genes (4345 ORFs) are shown in Figure 7A, while results for solely the 11 isoprenoid biosynthesis genes are shown in Figure 7B. The correlation for the 11 isoprenoid biosynthesis genes is very high ($R^2$ value of 0.972; $p < 2.54 \times 10^{-8}$), while the correlation for the whole genome is lower ($R^2 = 0.777$). There were no significant correlations, either for the genome or for the isoprenoid biosynthesis genes, between the $\log_2$ expression ratios of **13** or fosmidomycin when compared to the combination **13**−fosmidomycin, carbenicillin, or ciprofloxacin ratios (Supporting Information, Figure S7).

While it could always be argued that **13** and fosmidomycin just happen to have potent activity against another unknown target (resulting in the high correlation in gene expression), this possibility seems remote since there are no other known targets for these inhibitors, they have low nM $K_i$ values (against FPPS, DXR), and they show strong synergism (as opposed to the additivity which might be expected for activity against another, unknown target; **13** has no activity versus UPPS, OPPS or DXR; and fosmidomycin has no activity versus FPPS). In addition, as described above, the $IC_{50}$ values for **13** against *E. coli* overexpressing FPPS and for fosmidomycin overexpressing DXR are highly elevated, and in general the *E. coli* FPPS and cell growth inhibition data are correlated (for the compounds having measurable activity).

On the basis of these results, it is clear that some bisphosphonates are active against *E. coli* cell growth. The most potent compounds are all phenylalkyl nitrogen-containing bisphosphonates, known to be potent inhibitors of the FPPS enzyme (with potent activity also in bone resorption[41]). The most potent inhibitor, **13**, exhibits strong synergism with the DXR inhibitor fosmidomycin, and we find a high similarity in up- and down-regulated genes (Figures 6A, 7A) on treatment of *E. coli* K12 with these inhibitors, together with a remarkably similar pattern in gene transcription for all of the genes encoding the enzymes of the isoprenoid biosynthesis pathway (Figures 6B, 7B). Both inhibitors significantly up-regulate *dxr* (DXR, the target for fosmidomycin) and *uppS* (UPPS, a polyisoprenoid involved in cell wall biosynthesis that uses FPP as its substrate) but down-regulate *dxs* (DXS), *ispA* (FPPS), and *ispB* (OPPS). DXR and UPPS are considered to be essential enzymes in the isoprenoid biosynthesis pathway,[2,45] but interestingly, FPPS was recently found to be nonessential in *E. coli* since UPPS/OPPS can condense DMAPP and IPP into FPP,[46] albeit at a very slow rate.

On inhibition by fosmidomycin, cells up-regulate the transcription of *dxr*, to raise the amount of functional DXR. In addition, *uppS* is also up-regulated, reflecting most likely its key role in cell wall biosynthesis. With the bisphosphonate **13**, the gene transcription results obtained are very similar to those seen with fosmidomycin. This at first sight seems surprising, since it might be anticipated that FPPS inhibition would result in up-regulation of *ispA*, but *ispA* is actually slightly down-regulated, while *dxr* and *uppS* are strongly up-regulated. Fortunately, however, these results can be readily interpreted on the basis of the observation that the *E. coli ispA* disruptant is viable, using OPPS/UPPS to synthesize FPP from DMAPP and IPP.[46] So, instead of up-regulating *ispA* on bisphosphonate inhibition, the alternative route of up-regulating *uppS* (to make FPP, as well as the UPP required for lipid II/cell wall biosynthesis) occurs. Since **13** has no effect on *E. coli* UPPS activity in vitro (unpublished data), the up-regulation of *uppS* is related to isoprenoid pathway regulation and not to an inhibitory effect of **13** on UPPS. Likewise, **13** has no effect on DXR, and fosmidomycin has no effect on FPPS. The correlation ($R^2 = 0.972$, $p < 2.54 \times 10^{-8}$) in relative gene expression levels between the two inhibitors for the 11 isoprenoid biosynthesis genes is, therefore, remarkable and suggests that inhibition of different enzymes on the isoprenoid biosynthesis pathway induces the transcription of the same essential genes (*dxr*, *uppS*), in order to preserve isoprenoid homeostasis and maintain cell viability. The observation that *ispB* (OPPS) is the most down-regulated gene in both **13** and fosmidomycin treatments correlates well with the very low level of ubiquinone-8 (13%) and menaquinone-8 (18%) in null *ispA* mutants,[46] while the levels

of UPP are quite high in the disruptant (40−70%, depending on growth conditions), indicating that cells favor cell wall biosynthesis over quinone production when isoprenoid biosynthesis is inhibited (either by FPPS inhibition or genetically).

From a drug discovery perspective, the observation of a strong synergism between the phosphonate drug fosmidomycin (DXR inhibitor) and the bisphosphonate **13** (FPPS inhibitor) is of interest since it is a "proof-of-principle" that there can be strongly synergistic interactions between different isoprenoid biosynthesis pathway inhibitors in bacteria, just as there are in protozoa, yeasts, and fungi. Moreover, there is no requirement for the two targets to be immediately adjacent to each other in the metabolic pathway, as also noted previously in protozoa.[15] The dramatic effects observed with the combination **13**−fosmidomycin in the DNA microarray experiments (Figure 6) also help to explain the strongly synergistic interactions seen in the growth inhibition assays (Figure 4, Table 3), with the combination results obtained in the microarray closely resembling the effects seen with the potent antibiotic ciprofloxacin. The combination of **13**−fosmidomycin is highly toxic to *E. coli* K12 and there is clearly a very different response seen with the combination from that seen with **13** or fosmidomycin acting alone. Specifically, with the combination, we find that five isoprenoid biosynthesis genes—*dxs*, *ispG*, *ispH*, *idi*, *ispA*—are up-regulated, a very different picture from that seen with **13** and fosmidomycin acting alone (Figure 6, Supporting Information, Table S4). The effect is surprising since both the *idi* gene product (the DMAPP/IPP isomerase) as well as FPPS (*ispA*) are nonessential in *E. coli*.[46,47] Under two-drug pressure, however, *idi* is now up-regulated, as is *ispA*, suggesting that either the *uppS* route is no longer effective for FPP formation or, perhaps more likely, that there is an even more pressing need for IPP (to make UPP), which can be obtained via the *idi* gene product. The *idi* gene is not clustered to any other isoprenoid biosynthesis genes, and although its product, DMAPP/IPP isomerase, is not essential, it could help *E. coli* optimize utilization of DMAPP and IPP under stress conditions. Also of interest is the observation that both the *ispA* and *dxs* genes are located on the same (*xseB-ispA-dxs-yajO*) operon, which could help explain their common up-regulation by the combination **13**−fosmidomycin, due to cotranscription, and their common down-regulation by **13** and fosmidomycin acting alone.

The regulation of ubiquinone-8 and menaquinone-8 biosynthesis genes was also observed with **13**, fosmidomycin, and the combination **13**−fosmidomycin (Supporting Information, Table S4), but neither **13** nor fosmidomycin acting alone affected the transcription of the peptidoglycan biosynthesis genes (Supporting Information, Table S5). However, with the **13**−fosmidomycin combination, a high percentage of the peptidoglycan biosynthesis genes (involved in cell wall biosynthesis and survival) were up-regulated, consistent with the potent synergistic action of the drug combination. Likewise, neither **13** nor fosmidomycin had any effect on 53 genes responsible for DNA replication (Supporting Information, Table S6), but 18 of these genes were affected by the combination **13**−fosmidomycin, consistent again with the potent bactericidal effect of the drug combination. The efficacy of the combination treatment is also reflected in a similar SOS response to that observed with ciprofloxacin (Supporting Information, Table S7): many SOS response genes were up-regulated by the combination **13**−fosmidomycin and by ciprofloxacin, but few were up-regulated by **13** or carbenicillin, and none were affected by fosmidomycin, again reflecting the potent synergistic effect of the combination treatment.

## Conclusions

The results we have presented above are of interest for a number of reasons. First, we tested a library of 117 bisphosphonates for activity against *E. coli* W3110 growth inhibition, finding that the most potent inhibitors were those containing large arylalkyl side chains. These compounds are known to be potent inhibitors of bone resorption and FPPS. Second, we used common feature modeling to investigate cell growth inhibition as well as *E. coli* FPPS inhibition. The results showed the importance of having a distal hydrophobic feature for cell growth inhibition, due perhaps to enhanced cell uptake, and provided an explanation for the lack of activity of other potent bone resorption drugs, such as zoledronate and risedronate, which lack this feature but which still inhibit *E. coli* FPPS in vitro. Third, we found that the most potent bisphosphonate (**13**) acted in a strongly synergistic manner with fosmidomycin, a known inhibitor of the MEP pathway enzyme DXR, against *E. coli* K12. This synergism correlated with the enhanced bactericidal activity of the combination. Fourth, we found that fosmidomycin and **13** exert very similar effects on gene transcription. The correlation is genome-wide, but regulation of the 11 enzymes involved in isoprenoid biosynthesis (*dxs*, *dxr*, *ispD*, *ispE*, *ispF*, *ispG*, *ispH*, *idi*, *ispA*, *ispB*, *uppS*) is particularly highly correlated ($R^2 = 0.972$, $N = 11$, $p < 2.54 \times 10^{-8}$), suggesting the presence of isoprenoid biosynthesis homeostasis. Fifth, we used Venn diagram and a hierarchical cluster analyses to support this picture of a synergistic interaction, with the drug combinations showing potent antibacterial effects similar to those found with ciprofloxacin. Overall, these results are of general interest since they show that large, relatively hydrophobic bisphosphonates are inhibitors of *E. coli* cell growth, in addition to suggesting that drug combinations targeting different steps in isoprenoid biosynthesis in bacteria may lead to the development of novel, effective antibiotics.

**Acknowledgment.** This work was supported by the United States Public Health Service (NIH grant GM073216-26 to E.O. and AR45504 to C.T.M.). A.L. was supported by an NIH Institutional NRSA in Molecular Biophysics (NIH training grant GM-08276). D.S. was supported by a Howard Hughes Undergraduate Research Fellowship. We also thank Dr. Divyen Patel of Genome Exploration, Inc. (Memphis, TN), for conducting the Affymetrix GeneChip hybridization and for providing helpful comments. We thank Andy Wang for providing inhibition results for **13** against OPPS and UPPS, Jochen Wiesner for testing **13** against *E. coli* DXR, Shunsuke Yajima and Tomohisa Kuzuyama for providing their *E. coli* DXR expression system, Pavan Srinath for the FPPS inhibition results, and Takeda San Diego, Inc., for providing the *E. coli* FPPS expression system.

**Supporting Information Available:** Additional results, including growth inhibition, SAR, gene expression, Loewe additivity, and isobologram data. This material is available free of charge via the Internet at http://pubs.acs.org. Also, CEL files containing microarray experimental raw data are available free of charge via the Internet at http://feh.scs.uiuc.edu/data.

## References

(1) Projan, S. J.; Shlaes, D. M. Antibacterial drug discovery: Is it all downhill from here? *Clin. Microbiol. Infect.* **2004**, *10*, 18−22.
(2) Apfel, C. M.; Takacs, B.; Fountoulakis, M.; Stieger, M.; Keck, W. Use of genomics to identify bacterial undecaprenyl pyrophosphate synthetase: Cloning, expression, and characterization of the essential *uppS* gene. *J. Bacteriol.* **1999**, *181*, 483−492.
(3) Kato, J.; Fujisaki, S.; Nakajima, K.; Nishimura, Y.; Sato, M.; Nakano, A. The *Escherichia coli* homologue of yeast RER2t2, a key enzyme of dolichol synthesis, is essential for carrier lipid formation in bacterial cell wall synthesis. *J. Bacteriol.* **1999**, *181*, 2733−2738.

(4) Li, H.; Huang, J.; Jiang, X.; Seefeld, M.; McQueney, M.; Macarron, R. The effect of triton concentration on the activity of undecaprenyl pyrophosphate synthase inhibitors. *J. Biomol. Screen.* **2003**, *8*, 712−715.
(5) Liu, G. Y.; Essex, A.; Buchanan, J. T.; Datta, V.; Hoffman, H. M.; Bastian, J. F.; Fierer, J.; Nizet, V. *Staphylococcus aureus* golden pigment impairs neutrophil killing and promotes virulence through its antioxidant activity. *J. Exp. Med.* **2005**, *202*, 209−215.
(6) Kuntz, L.; Tritsch, D.; Grosdemange-Billiard, C.; Hemmerlin, A.; Willem, A.; Bach, T. J.; Rohmer, M. Isoprenoid biosynthesis as a target for antibacterial and antiparasitic drugs: Phosphonohydroxamic acids as inhibitors of deoxyxylulose phosphate reducto-isomerase. *Biochem. J.* **2005**, *386*, 127−135.
(7) Wilding, E. I.; Kim, D. Y.; Bryant, A. P.; Gwynn, M. N.; Lunsford, R. D.; McDevitt, D.; Myers, J. E., Jr.; Rosenberg, M.; Sylvester, D.; Stauffacher, C. V.; Rodwell, V. W. Essentiality, expression, and characterization of the class II 3-hydroxy-3-methylglutaryl coenzyme A reductase of *Staphylococcus aureus*. *J. Bacteriol.* **2000**, *182*, 5147−5152.
(8) Sacchettini, J. C., Poulter, C. D. Creating isoprenoid diversity. *Science* **1997**, *277*, 1788−1789.
(9) Rohmer, M. The discovery of a mevalonate-independent pathway for isoprenoid biosynthesis in bacteria, algae and higher plants. *Nat. Prod. Rep.* **1999**, *16*, 565−574.
(10) Jomaa, H.; Wiesner, J.; Sanderbrand, S.; Altincicek, B.; Weidemeyer, C.; Hintz, M.; Turbachova, I.; Eberl, M.; Zeidler, J.; Lichtenthaler, H. K.; Soldati, D.; Beck, E. Inhibitors of the nonmevalonate pathway of isoprenoid biosynthesis as antimalarial drugs. *Science* **1999**, *285*, 1502−1503.
(11) Liu, G. Y.; Doran, K. S.; Lawrence, T.; Turkson, N.; Puliti, M.; Tissi, L.; Nizet, V. Sword and shield: Linked group B streptococcal beta-hemolysin/cytolysin and carotenoid pigment function to subvert host phagocyte defense. *Proc. Natl. Acad. Sci. U.S.A.* **2004**, *101*, 14491−14496.
(12) Neu, H. C.; Kamimura, T. Synergy of fosmidomycin (FR-31564) and other antimicrobial agents. *Antimicrob. Agents Chemother.* **1982**, *22*, 560−563.
(13) Wiesner, J.; Henschker, D.; Hutchinson, D. B.; Beck, E.; Jomaa, H. In vitro and in vivo synergy of fosmidomycin, a novel antimalarial drug, with clindamycin. *Antimicrob. Agents Chemother.* **2002**, *46*, 2889−2894.
(14) Borrmann, S.; Adegnika, A. A.; Moussavou, F.; Oyakhirome, S.; Esser, G.; Matsiegui, P.-B.; Ramharter, M.; Lundgren, I.; Kombila, M.; Issifou, S.; Hutchinson, D.; Wiesner, J.; Jomaa, H.; Kremsner, P. G. Short-course regimens of artesunate-fosmidomycin in treatment of uncomplicated *Plasmodium falciparum* malaria. *Antimicrob. Agents Chemother.* **2005**, *49*, 3749−3754.
(15) Urbina, J. A.; Lazardi, K.; Marchan, E.; Visbal, G.; Aguirre, T.; Piras, M. M.; Piras, R.; Maldonado, R. A.; Payares, G.; de Souza, W. Mevinolin (Lovastatin) potentiates the antiproliferative effects of ketoconazole and terbinafine against *Trypanosoma (Schizotrypanum) cruzi*: In vitro and in vivo studies. *Antimicrob. Agents Chemother.* **1993**, *37*, 580−591.
(16) Martin, M. B.; Grimley, J. S.; Lewis, J. C.; Heath, H. T., III; Bailey, B. N.; Kendrick, H.; Yardley, V.; Caldera, A.; Lira, R.; Urbina, J. A.; Moreno, S. N.; Docampo, R.; Croft, S. L.; Oldfield, E. Bisphosphonates inhibit the growth of *Trypanosoma brucei*, *Trypanosoma cruzi*, *Leishmania donovani*, *Toxoplasma gondii*, and *Plasmodium falciparum*: A potential route to chemotherapy. *J. Med. Chem.* **2001**, *44*, 909−916.
(17) Benaim, G.; Sanders, J. M.; Garcia-Marchan, Y.; Colina, C.; Lira, R.; Caldera, A. R.; Payares, G.; Sanoja, C.; Burgos, J. M.; Leon-Rossell, A.; Concepcion, J. L.; Schijman, A. G.; Levin, M.; Oldfield, E.; Urbina, J. A. Amiodarone has intrinsic anti-*Trypanosoma cruzi* activity and acts synergistically with posaconazole. *J. Med. Chem.* **2006**, *49*, 892−899.
(18) Montalvetti, A.; Bailey, B. N.; Martin, M. B.; Severin, G. W.; Oldfield, E.; Docampo, R. Bisphosphonates are potent inhibitors of *Trypanosoma cruzi* farnesyl pyrophosphate synthase. *J. Biol. Chem.* **2001**, *276*, 33930−33937.
(19) Szabo, C. M.; Matsumura, Y.; Fukura, S.; Martin, M. B.; Sanders, J. M.; Sengupta, S.; Cieslak, J. A.; Loftus, T. C.; Lea, C. R.; Lee, H. J.; Koohang, A.; Coates, R. M.; Sagami, H.; Oldfield, E. Inhibition of geranylgeranyl diphosphate synthase by bisphosphonates and diphosphates: A potential route to new bone antiresorption and antiparasitic agents. *J. Med. Chem.* **2002**, *445*, 2185−2196.
(20) Martin, M. B.; Sanders, J. M.; Kendrick, H.; de Luca-Fradley, K.; Lewis, J. C.; Grimley, J. S.; Van Brussel, E. M.; Olsen, J. R.; Meints, G. A.; Burzynska, A.; Kafarski, P.; Croft, S. L.; Oldfield, E. Activity of bisphosphonates against *Trypanosoma brucei rhodesiense*. *J. Med. Chem.* **2002**, *45*, 2904−2914.
(21) Sanders, J. M.; Gomez, A. O.; Mao, J.; Meints, G. A.; Van Brussel, E. M.; Burzynska, A.; Kafarski, P.; Gonzalez-Pacanowska, D.; Oldfield, E. 3-D QSAR investigations of the inhibition of *Leishmania major* farnesyl pyrophosphate synthase by bisphosphonates. *J. Med. Chem.* **2003**, *46*, 5171−5183.
(22) Ghosh, S.; Chan, J. M.; Lea, C. R.; Meints, G. A.; Lewis, J. C.; Tovian, Z. S.; Flessner, R. M.; Loftus, T. C.; Burchhaus, I.; Kendrick, H.; Croft, S. L.; Kemp, R. G.; Kobayashi, S.; Nozaki, T.; Oldfield, E. Effects of bisphosphonates on the growth of *Entamoeba histolytica* and *Plasmodium* species in vitro and in vivo. *J. Med. Chem.* **2004**, *47*, 175−187.
(23) Sanders, J. M.; Ghosh, S.; Chan, J. M.; Meints, G.; Wang, H.; Raker, A. M.; Song, Y.; Colantino, A.; Burzynska, A.; Kafarski, P.; Morita, C. T.; Oldfield, E. Quantitative structure-activity relationships for $\gamma\delta$ T cell activation by bisphosphonates. *J. Med. Chem.* **2004**, *47*, 375−384.
(24) Ling, Y.; Sahota, G.; Odeh, S.; Chan, J. M.; Araujo, F. G.; Moreno, S. N.; Oldfield, E. Bisphosphonate inhibitors of *Toxoplasma gondi* growth: In vitro, QSAR, and in vivo investigations. *J. Med. Chem.* **2005**, *48*, 3130−3140.
(25) Kotsikorou, E.; Song, Y.; Chan, J. M.; Faelens, S.; Tovian, Z.; Broderick, E.; Bakalara, N.; Docampo, R.; Oldfield, E. Bisphosphonate inhibition of the exopolyphosphatase activity of the *Trypanosoma brucei* soluble vacuolar pyrophosphatase. *J. Med. Chem.* **2005**, *48*, 6128−6129.
(26) Bauer, A. W.; Kirby, W. M.; Sherris, J. C.; Turck, M. Antibiotic susceptibility testing by standardized single disk method. *Am. J. Clin. Pathol.* **1966**, *45*, 493−497.
(27) Kaneda, K.; Kuzuyama, T.; Takagi, M.; Hayakawa, Y.; Seto, H. An unusual isopentenyl diphosphate isomerase found in the mevalonate pathway gene cluster from *Streptomyces sp.* strain CL190. *Proc. Natl. Acad. Sci. U.S.A.* **2001**, *98*, 932−937.
(28) National Committee for Clinical Laboratory Standards. *Methods for dilution antimicrobial susceptibility tests for bacteria that grow aerobically. Approved Standard, 5th ed.;* NCCLS document M7−A5; National Committee for Clinical Laboratory Standards: Wayne, PA, 2000.
(29) American Type Culture Collection. MTT Cell Proliferation Assay. ATCC, Manassas, VA. http://www.atcc.org/documents/odf/20-1010.k.pdf, 2001 [online].
(30) Rieger, C. E.; Lee, J.; Turnbull, J. L. A continuous spectrophotometric assay for aspartate transcarbamylase and ATPases. *Anal. Biochem.* **1997**, *246*, 86−95.
(31) Eliopoulos, G. M.; Moellering, R. C. Antimicrobial combinations. In *Antibiotics in Laboratory Medicine*, 4th ed.; Lorian, V., Ed.; Williams & Wilkins Publising Co.: Baltimore, 1998; pp 330−396.
(32) Singh, P. K.; Tack, B. F.; McCray, P. B.; Welsh, M. J. Synergistic and additive killing by antimicrobial factors found in human airway surface liquid. *Am. J. Physiol. Lung Cell Mol. Physiol.* **2000**, *279*, 799−805.
(33) European Committee for Antimicrobial Susceptibility Testing (EUCAST) of the European Society of Clinical Microbiology and Infectious Diseases (ESCMID). EUCAST Definitive Document E. Def 1.2, May 2000: Terminology relating to methods for the determination of susceptibility of bacteria to antimicrobial agents. *Clin. Microbiol. Infect.* **2000**, *6*, 503−508.
(34) Suhnel, J. Zero interaction response surfaces, interaction functions and difference response surfaces for combinations of biologically active agents. *Arzneim.-Forsch.* **1992**, *42*, 1251−1258.
(35) Berenbaum, M. C. What is synergy? *Pharmacol. Rev.* **1989**, *41*, 93−141.
(36) Tel-Test, Inc. 2004. RNA STAT-60. Total RNA/mRNA isolation reagent. Tel-Test, Inc., Friendswood, TX. http://www.isotexdiagnostics.com/rna_stat-60_reagent.html [online].
(37) Affymetrix, Inc. 2002. GeneChip *E. coli* antisense genome array technical manual. Affymetrix, Inc., Santa Clara, CA. http://www.affymetrix.com/support/technical/manuals.affx [online].
(38) Li, C.; Wong, W. H. Model-based analysis of oligonucleotide arrays: Model validation, design issues and standard error application. *Genome Biology* **2001**, *2*:research0032.1−0032.11 [online].
(39) Chu, T.; Weir, B.; Wolfinger, R. A systematic statistical linear modeling approach to oligonucleotide array experiments. *Math. Biosci.* **2002**, *176*, 35−51.
(40) Takagi, M.; Kuzuyama, T.; Takahashi, S.; Seto, H. A gene cluster for the mevalonate pathway from *Streptomyces sp.* Strain CL190. *J. Bacteriol.* **2000**, *182*, 4153−4157.
(41) Widler, L.; Jaeggi, K. A.; Glatt, M.; Muller, K.; Bachmann, R.; Bisping, M.; Born, A. R.; Cortesi, R.; Guiglia, G.; Jeker, H.; Klein, R.; Ramseier, U.; Schmid, J.; Schreiber, G.; Seltenmeyer, Y.; Green, J. R. Highly potent geminal bisphosphonates. From pamidronate disodium (Aredia) to zoledronic acid (Zometa). *J. Med. Chem.* **2002**, *45*, 3721−3738.

(42) Kotsikorou, E.; Oldfield, E. A quantitative structure-activity relationship and pharmacophore modeling investigation of aryl-X and heterocyclic bisphosphonates as bone resorption agents. *J. Med. Chem.* **2003**, *46*, 2932−2944.
(43) Buckner, F. E.; Griffin, J. H.; Wilson, A. J.; Van Voorhis, W. C. Potent anti-*Trypanosoma cruzi* activities of oxidosqualene cyclase inhibitors. *Antimicrob. Agents Chemother*. **2001**, *45* (4), 1210−1215.
(44) Shaw, K. J.; Miller, N.; Liu, X.; Lerner, D.; Wan, J.; Bittner, A.; Morrow, B. J. Comparison of the changes in global gene expression of *Escherichia coli* induced by four bactericidal agents. *J. Mol. Microbiol. Biotechnol.* **2003**, *5*, 105−122.
(45) Takahashi, S.; Kuzuyama, T.; Watanabe, H.; Seto, H. A 1-deoxy-D-xylulose 5-phosphate reductoisomerase catalyzing the formation of 2-C-methyl-D-erythriol 4-phosphate in an alternative nonmevalonate pathway for terpenoid biosynthesis. *Proc. Natl. Acad. Sci. U.S.A.* **1998**, *95*, 9879−9884.
(46) Fujisaki, S.; Takahashi, I.; Hara, H.; Horiuchi, K.; Nishino, T.; Nishimura, Y. Disruption of the structural gene for farnesyl diphosphate synthase in *Escherichia coli*. *J. Biochem. (Tokyo)* **2005**, *137*, 395−400.
(47) Hahn, F. M.; Hurlburt, A. P.; Poulter, C. D. *Escherichia coli* open reading frame 696 is idi, a nonessential gene encoding isopentenyl diphosphate isomerase. *J. Bacteriol.* **1999**, *181*, 4499−4504.

JM060492B